

# Wind Energy Conversion Systems for Direct-Drive PMSG Based On Discrete-Time Direct Torque Control with Fuzzy Logic

Basireddy Manitejanath Reddy<sup>#1</sup>, M Paramesh<sup>\*2</sup>

<sup>#</sup>M. Tech student, GATES Institute of Technology, Gooty, Andhrapradesh, India

<sup>\*</sup>Associate Professor, Dept. of EEE

GATES Institute of Technology, Gooty, Andhrapradesh, India

**Abstract**— This project proposes a fuzzy logic based discrete-time direct torque control (DTC) scheme for salient-pole permanent-magnet synchronous generators (PMSGs) used in the variable-speed, direct-drive wind energy conversion systems (WECSs). The discrete-time control law is derived from the perspective of flux space vectors and load angle with the torque and stator flux information only. The saliency of the PMSG is eliminated by the active flux concept. Compared with the existing space vector modulation (SVM)-based DTCs, the proposed scheme removes the use of PI regulators and use fuzzy controller for error reduction purpose and is less dependent on the machine parameters, e.g., stator inductances and permanent-magnet flux linkage, while maintaining the fast dynamic response of the system. By integrating the SVM into the control scheme, the torque and flux ripples are greatly reduced and the switching frequency becomes fixed. The effectiveness of the proposed DTC scheme is verified by real-time simulations implemented on an OPAL-RT real-time simulator and experimental results for a 180-W salient-pole PMSG used in a direct-drive WECS

can be connected directly to a wind turbine without the use of a gearbox, which significantly reduces the construction, operation, and maintenance costs of the WECSs [2], [3].

Typically, the control systems of PMSGs adopt a decoupled current control executed in a synchronized rotating reference frame. In the last few decades, an alternative electric machine control scheme called the direct torque control (DTC) has attracted extensive attention from both academia and industry. Different from the decoupled current control, the DTC directly controls electromagnetic torque and stator flux linkage instead of armature currents, hence possessing the merits of fast dynamic response, simple implementation, and high robustness to external disturbances. The DTC has been applied successfully in high-performance industrial servo drive systems [4]. For WECS applications, the DTC may facilitate the realization of MPPT with the optimal torque control [1], since the optimal torque command can be applied directly in the DTC without the need of wind speed measurements. In this way, the outer loop speed or power controller, which is necessary in the decoupled current control, can be eliminated [5].

**Index Terms**— Direct torque control (DTC), flux space vector, load angle analysis, permanent-magnet synchronous generator (PMSG), wind energy conversion system (WECS).

In the conventional DTC, the voltage vector commands are determined primarily by the outputs of two hysteresis comparators. Once selected, the desired voltage vector will remain unchanged until the hysteresis states are updated. Although this voltage modulation scheme is simple to execute, it will lead to irregular and unpredictable torque and flux ripples, particularly when the DTC is applied on a digital platform [6]. To solve these problems, many approaches have been developed from different perspectives. One natural thought is to increase the number of available voltage vectors, e.g., using multilevel converters [7], [8] or equally dividing the sampling period into multiple intervals [9]. However, these methods will increase the hardware cost, need additional prediction for rotor speed, or have a limited ripple reduction improvement. Another effective technique is to integrate the space vector modulation (SVM) algorithm into the DTC [10]–[15]. The SVM is able to convert the input voltages into gate signals for the inverter using a fixed switching frequency. A variety of SVM-based DTC schemes have been

## I. Introduction

OVER the last two decades, the increasing concerns on energy crisis and environmental pollutions have significantly promoted the utilization of renewable energy. Among various renewable energy sources, wind energy has become one of the most cost-effective sources for electricity generation. The variable-speed wind energy conversion systems (WECSs), which can be operated in the maximum power point tracking (MPPT) mode, have attracted considerable interests, owing to their high energy production efficiency and low torque spikes [1]. Among different types of generators, the permanent-magnet synchronous generators (PMSGs) have been found superior, owing to their advantages such as high power density, high efficiency, and high reliability. Furthermore, a PMSG with a high number of poles

investigated for permanent-magnet synchronous machines (PMSMs) in the last few decades. In general, they can be classified into two categories based on how the voltage references are generated in the stationary reference frame. In the first category, the decoupled voltage references in the synchronously rotating reference frame are acquired and then transformed to the stationary reference frame using the rotary coordinate transformation [12]–[14]. In the second category, the voltage references are obtained directly from the incremental stator flux vectors in the stationary reference frame without coordinate transformation [15].

Both methods can reduce torque and flux ripples, but need proportional–integral (PI) controllers to regulate the torque and stator flux errors. The PI gains are usually tuned by a trial-and-error procedure [12]. Poorly tuned PI gains will deteriorate the dynamic performance of the DTC. In addition, according to [9], a real DTC scheme should not contain PI regulators. More recently, a predictive current control [16], [17] and a deadbeat direct torque and flux control [18] were investigated for surface-mounted and interior PMSMs. These control schemes provide good dynamic performance, provided that the information of some machine parameters, e.g., stator inductances and permanent-magnet flux linkage, is accurate. Therefore, the performance of the control systems would be more or less influenced by the variations of the machine parameters. Moreover, these control schemes are based on the inverse machine model or a graphical method, which increase the computational complexity. This paper proposes a discrete-time SVM-based DTC without PI regulators for direct-drive PMSG-based WECSs. The discrete-time control law is derived from the prospective of flux space vectors and load angle. Several machine parameters, e.g., stator inductances and permanent-magnet flux linkage, are not presented in the control law. This improves the robustness of the control system to PMSG parameter variations. By adopting the proposed DTC scheme, the torque and flux ripples are reduced, and the fast dynamic response is retained when compared with the conventional DTC scheme. The proposed DTC scheme is validated by simulation and experimental results for a 2.4-kW nonsalient-pole PMSG and a 180-W salient-pole PMSG used in the direct-drive WECSs.

## II. Permanent Magnet Synchronous Generator

A permanent magnet synchronous generator is a generator where the excitation field is provided by a permanent magnet instead of a coil. The term synchronous refers here to the fact that the rotor and magnetic field rotate with the same speed, because the magnetic field is generated through a shaft mounted permanent magnet mechanism and current is induced into the stationary armature

Synchronous generators are the majority source of commercial electrical energy. They are commonly used to convert the mechanical power output of steam turbines, gas turbines, reciprocating engines and hydro turbines into electrical power for the grid. Wind turbines of any significant scale use asynchronous generators exclusively

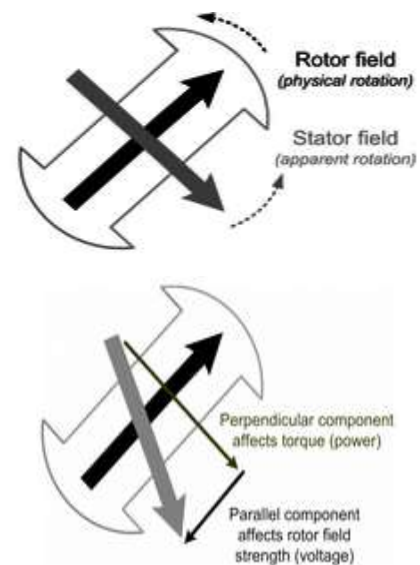


Fig 1: Permanent magnet synchronous generator

In the majority of designs the rotating assembly in the center of the generator—the "rotor"—contains the magnet, and the "stator" is the stationary armature that is electrically connected to a load. As shown in the diagram above, the perpendicular component of the stator field affects the torque while the parallel component affects the voltage. The load supplied by the generator determines the voltage. If the load is inductive, then the angle between the rotor and stator fields will be greater than 90 degrees which corresponds to an increased generator voltage. This is known as an overexcited generator. The opposite is true for a generator supplying a capacitive load which is known as an under excited generator. A set of three conductors make up the armature winding in standard utility equipment, constituting three phases of a power circuit—that correspond to the three wires we are accustomed to see on transmission lines. The phases are wound such that they are 120 degrees apart spatially on the stator, providing for a

uniform force or torque on the generator rotor. The uniformity of the torque arises because the magnetic fields resulting from the induced currents in the three conductors of the armature winding combine spatially in such a way as to resemble the magnetic field of a single, rotating magnet. This stator magnetic field or "stator field" appears as a steady rotating field and spins at the same frequency as the rotor when the rotor contains a single dipole magnetic field. The two fields move in "synchronicity" and maintain a fixed position relative to each other as they spin.<sup>[1]</sup>

They are known as synchronous generators because  $f$ , the frequency of the induced voltage in the stator (armature conductors) conventionally measured in hertz, is directly proportional to RPM, the rotation rate of the rotor usually given in revolutions per minute (or angular speed). If the rotor windings are arranged in such a way as to produce the effect of more than two magnetic poles, then each physical revolution of the rotor results in more magnetic poles moving past the armature windings. Each passing of a north and south pole corresponds to a complete "cycle" of a magnet field oscillation. Therefore, the constant of proportionality is  $\frac{1}{P}$ , where  $P$  is the number of magnetic rotor poles (almost always an even number), and the factor of 120 comes from 60 seconds per minute and two poles in a single magnet; The power in the prime mover is a function of RPM and torque. where is mechanical power in Watts, is the torque with units of  $\text{Nm}$ , and RPM is the rotations per minute which is multiplied by a factor of  $\frac{1}{60}$  to give units of  $\text{Hz}$ . By increasing the torque on the prime mover, a larger electrical power output can be generated.

### III. Wind Turbines with Permanent Magnet Synchronous Generator

Research about dynamic models for grid-connected wind energy conversion systems is one of the challenges to achieve knowledge for the on-going change due to the intensification of using wind energy in nowadays. This book chapter is an involvement on those models, but dealing with wind energy conversion systems consisting of wind turbines with permanent magnet synchronous generators (PMSG) and full-power converters. Particularly, the focus is on models integrating the dynamic of the system as much as potentially necessary in order to assert consequences on the operation of system. In modelling the energy captured from the wind by the blades, disturbance imposed by the asymmetry in the turbine, the vortex tower interaction, and the mechanical eigen swings in the blades are introduced in order to assert a more accurate behaviour of wind energy conversion systems. The conversion system

dynamic comes up from modelling the dynamic behaviour due to the main subsystems of this system: the variable speed wind turbine, the mechanical drive train, and the PMSG and power electronic converters. The mechanical drive train dynamic is considered by three different model approaches, respectively, onemass, two-mass or three-mass model approaches in order to discuss which of the approaches are more appropriated in detaining the behaviour of the system. The power electronic converters are modelled for three different topologies, respectively, two-level, multilevel or matrix converters. The consideration of these topologies is in order to expose its particular behaviour and advantages in what regards the total harmonic distortion of the current injected in the electric network. The electric network is modelled by a circuit consisting in a series of a resistance and inductance with a voltage source, respectively, considering two hypotheses: without harmonic distortion or with distortion due to the third harmonic, in order to show the influence of this third harmonic in the converter output electric current. Two types of control strategies are considered in the dynamic models of this book chapter, respectively, through the use of classical control or fractional-order control. Case studies were written down in order to emphasize the ability of the models to simulate new contributions for studies on grid-connected wind energy conversion systems.

### IV. PROJECT DESCRIPTION AND CONTROL DESIGN DIRECT-DRIVE PMSG-BASED WECS

The configuration of a direct-drive PMSG-based WECS is shown in Fig. 2, where the wind turbine is connected to the PMSG directly without a gearbox. The electrical power generated by the PMSG is transmitted to a power grid or supplied to a load via a variable-frequency power converter. Typically, the power electronic conversion system consists of a machine-side converter (MSC) and a grid-side converter (GSC) connected back-to-back via a dc link. This paper considers the standard power converter topology in a PMSG-based WECS, where both the MSC and the GSC are two-level fully controlled voltage source converters.

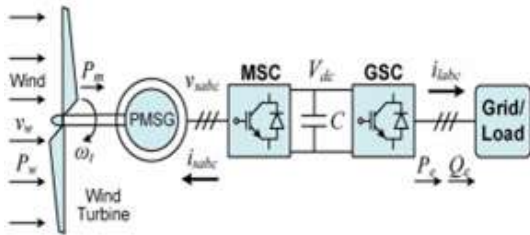


Fig2: Configuration of a direct drive PMSG-based WECS connected to the grid/load

### A. Wind Turbine Aerodynamic and Shaft Dynamic Models

The mechanical power that can be extracted from wind by a wind turbine is given by

$$P_m = \frac{1}{2} \rho A_r v_w^3 C_p(\lambda) = f(v_w, \omega_t) \quad (1)$$

where  $\rho$  is the air density;  $A_r$  is the area swept by the blades;  $v_w$  is the wind speed;  $C_p$  is the turbine power coefficient;  $\omega_t$  is the turbine shaft speed; and  $\lambda$  is the tip-speed ratio, which is defined by

$$\lambda = \frac{\omega_t r}{v_w} \quad (2)$$

where  $r$  is the radius of the wind turbine rotor plane. As the wind turbine is connected to the PMSG directly, the shaft system of the WECS can be represented by a one-mass model. The motion equation is then given by

$$2H \frac{d\omega_t}{dt} = \frac{P_m}{\omega_t} + \frac{P_e}{\omega_t} - D\omega_t \quad (3)$$

where  $2H$  is the total inertia constant of the WECS,  $P_e$  is the electric power generated by the PMSG, and  $D$  is the damping coefficient.

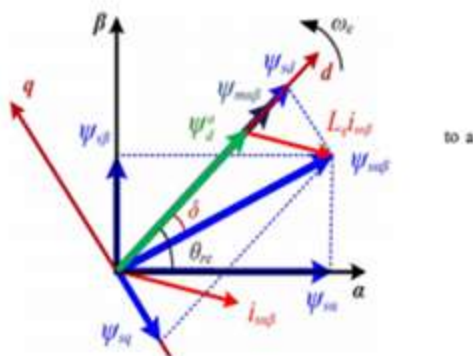


Fig3: Space vector diagram of fluxes and currents of PMSG.

### B. Modeling of the PMSG

The dynamic equations of a three-phase PMSG can be written in a synchronously rotating dq reference frame (see Fig. 2) as

$$\begin{bmatrix} v_{sd} \\ v_{sq} \end{bmatrix} = \begin{bmatrix} R_s + pL_d & -\omega_e L_q \\ \omega_e L_d & R_s + pL_q \end{bmatrix} \begin{bmatrix} i_{sd} \\ i_{sq} \end{bmatrix} + \begin{bmatrix} 0 \\ \omega_e \psi_m \end{bmatrix} \quad (4)$$

where  $p$  is the derivative operator;  $v_{sd}$  and  $v_{sq}$  are the d- and q-axis stator terminal voltages, respectively;  $i_{sd}$  and  $i_{sq}$  are the d- and q-axis stator currents, respectively;  $R_s$  is the resistance of the stator windings;  $L_d$  and  $L_q$  are the d- and q-axis inductances, respectively;  $\omega_e$  is the rotor electrical angular speed; and  $\psi_m$  is the flux linkage generated by the permanent magnets. The d- and q-axis stator flux linkages of the PMSG, i.e.,  $\psi_{sd}$  and  $\psi_{sq}$ , have the form of

$$\begin{bmatrix} \psi_{sd} \\ \psi_{sq} \end{bmatrix} = \begin{bmatrix} L_d & 0 \\ 0 & L_q \end{bmatrix} \begin{bmatrix} i_{sd} \\ i_{sq} \end{bmatrix} + \begin{bmatrix} \psi_m \\ 0 \end{bmatrix} \quad (5)$$

The electromagnetic torque  $T_e$  generated by the PMSG can be calculated by

$$T_e = \frac{3}{2} n \cdot \psi_m \cdot i_{sq} + \frac{3}{2} n (L_d - L_q) i_{sd} \cdot i_{sq} \quad (6)$$

where  $n$  is the number of pole pairs of the PMSG. The torque can also be expressed, in terms of stator flux linkage and load angle, as follows:

$$T_e = \frac{3}{2} \frac{n}{L_d} |\psi_s| \psi_m \sin \delta + \frac{3}{4} \frac{n}{L_d L_q} |\psi_s|^2 (L_d - L_q) \sin(2\delta) \quad (7)$$

where  $|\psi_s|$  is the magnitude of the stator flux vector, and  $\delta$  is the load angle. Both of the torque expressions (6) and (7) consist of two terms: The magnetic torque and the reluctance torque. Compared to a non-salient-pole PMSG ( $L_d = L_q$ ), a salient-pole PMSG can generate a higher torque with the same levels of  $i_{sd}$  and  $i_{sq}$ , owing to the rotor saliency ( $L_d \neq L_q$ ). However, the nonlinear reluctance torque in (7) complicates the mathematical relationship among  $T_e$ ,  $|\psi_s|$ , and  $\delta$ . In [1] and [2], an "active flux" concept was proposed to turn the salient-pole ac machines into nonsalient-pole ones, such that the reluctance torque and the magnetic torque were combined as one single term. The active flux magnitude  $|\psi_a|$  in [12] was defined as:

$$|\psi_a| = \psi_m + (L_d - L_q) i_{sd} \quad (8)$$

The idea can be extended to (7). Substituting isq from (5) into (6) gives

$$T_e = \frac{3}{2} n (\psi_m + (L_d - L_q) i_{sd}) \frac{\psi_{sq}}{L_q} \quad (9)$$

Since  $\psi_{sq} = |\psi_s| \cdot \sin \delta$ , the torque in terms of the stator flux magnitude, active flux magnitude, and load angle can be expressed as

$$T_e = \frac{3}{2} \frac{n}{L_q} |\psi_s| |\psi_d^a| \sin \delta \quad (10)$$

Dividing (7) by (10), the active flux magnitude in terms of  $|\psi_s|$  and  $\delta$  has the form of

$$|\psi_d^a| = \frac{L_q}{L_d} \left( \psi_m + \frac{|\psi_s|}{L_q} (L_d - L_q) \cos \delta \right) \quad (11)$$

The active flux vector  $\psi_{ad}$ , which is aligned on the d-axis, can be obtained by

$$\psi_d^a = \psi_{s\alpha\beta} - L_q i_{s\alpha\beta} \quad (12)$$

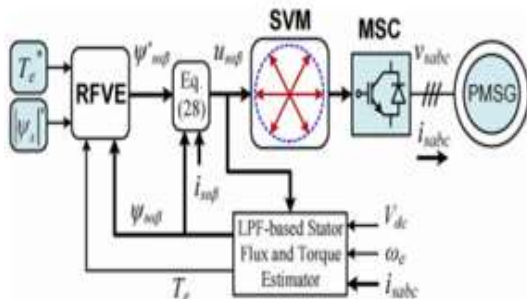


Fig4: Proposed DTC

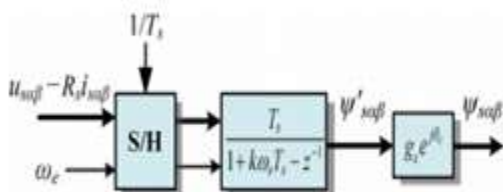


Fig5: Discrete time programmable LPF-based stator flux estimator

where  $\psi_{s\alpha\beta}$  and  $i_{s\alpha\beta}$  are the stator flux and current vectors in the stationary reference frame, respectively. The diagram in Fig. 3 illustrates the relationship between the fluxes and currents of the PMSG in the vector space, where  $\psi_{m\alpha\beta}$  is the rotor flux vector in the stationary reference frame.

## V. PROPOSED DISCRETE-TIME DTC

In the proposed DTC, all the calculations are executed in the stationary  $\alpha\beta$  reference frame. The schematic diagram of the proposed DTC is shown in Fig. 4. A reference flux vector estimator (RFVE) is designed to calculate the desired stator flux vector  $\psi^*_{s\alpha\beta}$  using the estimated and reference values of the stator flux and electromagnetic torque without PI regulators. In this paper, the stator flux linkages are estimated by the programmable low-pass filter (LPF) introduced in [9]. To effectively eliminate the dc drift over a wide speed range, the cutoff frequency of the LPF, i.e.,  $\omega_c$ , is adjusted according to the rotor electrical speed  $\omega_e$  by  $\omega_c = k \cdot \omega_e$ , where  $k$  is a constant. The schematic of the discrete-time programmable LPF-based stator flux estimator is shown in Fig. 4. The time derivative term is approximated by the Euler backward differentiation, which is given as

$$s = \frac{(1 - z^{-1})}{T_s} \quad (13)$$

where  $T_s$  is the sampling period, which is the same as the switching period and control cycle in the proposed DTC.

## VI. SIMULATION RESULTS

### A. System Setup Description

Simulation studies are carried out in MATLAB/Simulink to validate the proposed discrete-time DTC scheme for two PMSGs. The parameters of the two PMSGs are listed in Table I. The power rating of the salient-pole PMSG #1 is 180 W, and its dc-bus voltage is 41.75 V. The nonsalient-pole PMSG #2 is used in a practical direct-drive WECS (Sky stream 3.7) with a 2.4-kW rated power and a dc-bus voltage of 300 V. In the simulation, the value of  $k$  in (14) and (15) is set as  $1/\sqrt{2}$ . The sampling period is 100  $\mu$ s for both PMSG control systems, which is typically equal to one pulse width modulation (PWM) control cycle in practical applications. The dead time of the insulated gate bipolar transistors (IGBTs) in the MSC is set as 1  $\mu$ s and is compensated by the algorithm introduced in [22]. The performance comparison of the proposed DTC, the conventional DTC, and a stator flux-oriented SVM-DTC (named PI-DTC) in [12] is first investigated on PMSG #1. The conventional

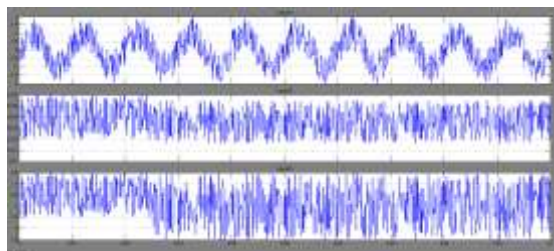
TABLE I  
PARAMETERS OF THE PMSGs

Parameter	PMSG #1	PMSG #2
Number of pole pairs $p$	4	21
Magnet flux linkage $\varphi_m$	0.01344 V·s	0.2532 V·s
Stator resistance $R_s$	0.235 $\Omega$	1.5 $\Omega$
$d$ -axis inductance $L_d$	0.275 mH	0.87 mH
$q$ -axis inductance $L_q$	0.364 mH	0.91 mH

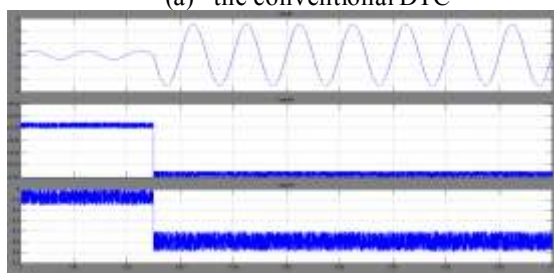
DTC in this paper is implemented by adopting the switching table in [10], where the torque error is regulated by a three-level torque hysteresis controller. The stator flux is estimated by using the PMSG current model in the stationary reference frame, which is given by

$$\begin{bmatrix} \psi_{\alpha} \\ \psi_{\beta} \end{bmatrix} = \begin{bmatrix} L + \Delta L \cos(2\theta_{re}) & \Delta L \sin(2\theta_{re}) \\ \Delta L \sin(2\theta_{re}) & L - \Delta L \cos(2\theta_{re}) \end{bmatrix} \begin{bmatrix} i_{\alpha} \\ i_{\beta} \end{bmatrix} + \psi_m \begin{bmatrix} \cos \theta_{re} \\ \sin \theta_{re} \end{bmatrix}$$

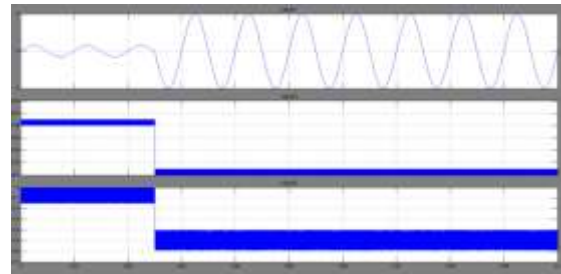
where  $L = (L_d + L_q)/2$  and  $\Delta L = (L_d - L_q)/2$ . The current-model-based stator flux estimator could achieve good performance in both steady and transient states, but needs more machine parameters compared to the voltage-model-based stator flux estimator used in the proposed DTC.



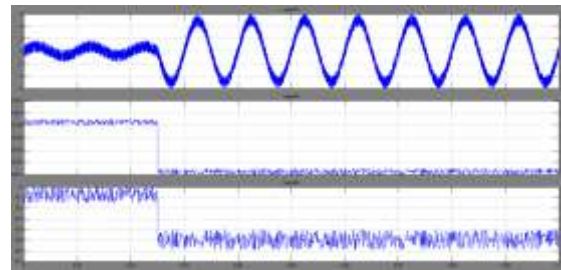
(a) the conventional DTC



(b) the PI-DTC



(c) the proposed DTC with a 10-kHz sampling frequency



(d) the conventional DTC with a 67-kHz sampling frequency (DTC-1).

**Fig6:** Dynamic responses of torque, stator flux magnitude, and instantaneous phase-A stator current of PMSG #1 using (a) the conventional DTC, (b) the PI-DTC, and (c) the proposed DTC with a 10-kHz sampling frequency as well as (d) the conventional DTC with a 67-kHz sampling frequency (DTC-1).

a distinct superiority in reducing the steady-state torque and stator flux magnitude ripples and stator current harmonics for different loading conditions. This is true even when the conventional DTC is implemented with a much higher sampling frequency (leading to a higher computational cost) so as to have an equivalent switching frequency same as the switching frequency of the proposed DTC and the PI-DTC.

## VII. CONCLUSION

This paper has proposed a novel discrete-time DTC based on flux space vectors for PMSGs used in direct-drive WECSs. The algorithm is easy to implement and is suitable for digital control systems using relatively low sampling frequencies. The torque and flux ripples have been significantly reduced with the integration of the SVM. In addition, the overall DTC scheme eliminated the use of PI controllers, showed strong robustness to machine parameter variations, and achieved fast dynamic responses. The proposed DTC scheme can be applied to salient-pole PMSGs. Simulation results have been carried out to validate the effectiveness of the proposed DTC scheme on a 180-W salient-pole PMSG.

## REFERENCES

- [1] Y. Zhao, C. Wei, Z. Zhang, and W. Qiao, "A review on position/speed sensorless control for permanent-magnet synchronous machine-based wind energy conversion systems," *IEEE J. Emerging Sel. Topics Power Electron.*, vol. 1, no. 4, pp. 203–216, Dec. 2013.
- [2] W. Qiao, L. Qu, and R. G. Harley, "Control of IPM synchronous generator for maximum wind power generation considering magnetic saturation," *IEEE Trans. Ind. Appl.*, vol. 45, no. 3, pp. 1095–1105, May/Jun. 2009.
- [3] W. Qiao, X. Yang, and X. Gong, "Wind speed and rotor position sensorless control for direct-drive PMG wind turbines," *IEEE Trans. Ind. Appl.*, vol. 48, no. 1, pp. 3–11, Jan./Feb. 2012.
- [4] *Direct Torque Control—The World's Most Advanced AC Drive Technology*, Tech. Guide No. 1, ABB, Zürich, Switzerland, Jun. 2011.
- [5] Z. Zhang, Y. Zhao, W. Qiao, and L. Qu, "A space-vector modulated sensorless direct-torque control for direct-drive PMSG wind turbines," *IEEE Trans. Ind. Appl.*, vol. 50, no. 4, pp. 2331–2341, Jul./Aug. 2014.
- [6] L. Zhong, M. F. Rahman, W. Y. Hu, and K. W. Lim, "Analysis of direct torque control in permanent magnet synchronous motor drives," *IEEE Trans. Power Electron.*, vol. 12, no. 3, pp. 528–536, May 1997.
- [7] C. A. Martins, X. Roboam, T. A. Meynard, and A. S. Carvalho, "Switching frequency imposition and ripple reduction in DTC drives by using a multilevel converter," *IEEE Trans. Power Electron.*, vol. 17, no. 2, pp. 286–297, Mar. 2002.
- [8] Y. Zhang, J. Zhu, Z. Zhao, W. Xu, and D. G. Dorrell, "An improved direct torque control for three-level inverter-fed induction motor sensorless drive," *IEEE Trans. Power Electron.*, vol. 27, no. 3, pp. 1502–1513, Mar. 2002.
- [9] D. Casadei, F. Profumo, and G. Serra, "FOC and DTC: Two viable schemes for induction motors torque control," *IEEE Trans. Power Electron.*, vol. 17, no. 5, pp. 779–787, Sep. 2002.
- [10] G. S. Buja and M. P. Kazmierkowski, "Direct torque control of PWM inverter-fed AD motors—A survey," *IEEE Trans. Ind. Electron.*, vol. 42, no. 4, pp. 344–350, Aug. 1995.